International Research Journal of Natural and Applied Sciences
ISSN: (2349-4077)
Impact Factor 5.46 Volume 4, Issue 7, July 2017
Website- www.aarf.asia, **Email** : editor@aarf.asia , editoraarf@gmail.com

Synthesis and characterization of Telluroether complexes of some Transition metal ion

by
Ashutosh Kumar,
Research scholar, JP university chapra

ABSTRACT:

This review traces the development and application of the tris(thioether)borate ligands, tripodal ligands with highly polarizable thioether donors. Areas of emphasis include the basic coordination chemistry of the mid-to-late first row transition metals (Fe, Ni, Co, Cu), and the role of the thioether substituent in directing complex formation, the modeling of zinc thiolate protein active sites, high-spin organo-iron and organo-cobalt chemistry, the preparation of monovalent complexes of Fe, Co and Ni, and dioxygen and sulfur activation by monovalent nickel complexes.

Keywords: Thioether, Borates, Nickel, Cobalt, Iron, Zinc, Dioxygen

1.INTRODUCTIONT

The development of polydentate ligands represents a central feature of modern synthetic chemistry with applications including coordination, supramolecular [1], organometallic and bioinorganic chemistry as well as catalyst development in areas as diverse as organic synthesis [2] and alternative energy production [3]. The ligand characteristics impact the resulting complex composition, structure and reactivity by controlling nuclearity, stereochemistry, spin states and the overall electronic structure of the metal ion. Further, while most attention has focused on attenuating the metal ion's primary coordination sphere, lessons from biology have inspired the development of rigid motifs that impinge on the second coordination sphere as well [4]. Among the most widely used polydentate ligands are tripodal frameworks that provide three donors in a facial arrangement. The archetype of this family is the cyclopentadienyl ligand (Cp) [5] and its relatives, e.g. pentamethylcyclopentadienyl (Cp*), ligands that were the genesis of modern organometallic chemistry. Cp is a pseudo-face capping ligand that binds as an anion providing six electrons. By a number of criteria the hydridotris(pyrazolyl)borates (Tp) [6] may be considered the second major member of the monoanionic tripodal ligand family. While isoelectronic with Cp ligands, the Tp donors afford significantly greater diversity due to the extensive range of pyrazole ring substituents that can be added [6]. One illustrative example is a comparison of the oxygen derivatives of $[Tp^{iPr2}]Cu$ and $[Tp^{tBu}]Cu$ (Fig. 1). Whereas, the former complex is dimeric with a μ-η^2:η^2-peroxo bridge [7], the

steric requirements of the 3-*tert*-butyl pyrazole substituents in the latter enforce a monomer, with side-on superoxide ligation [8].

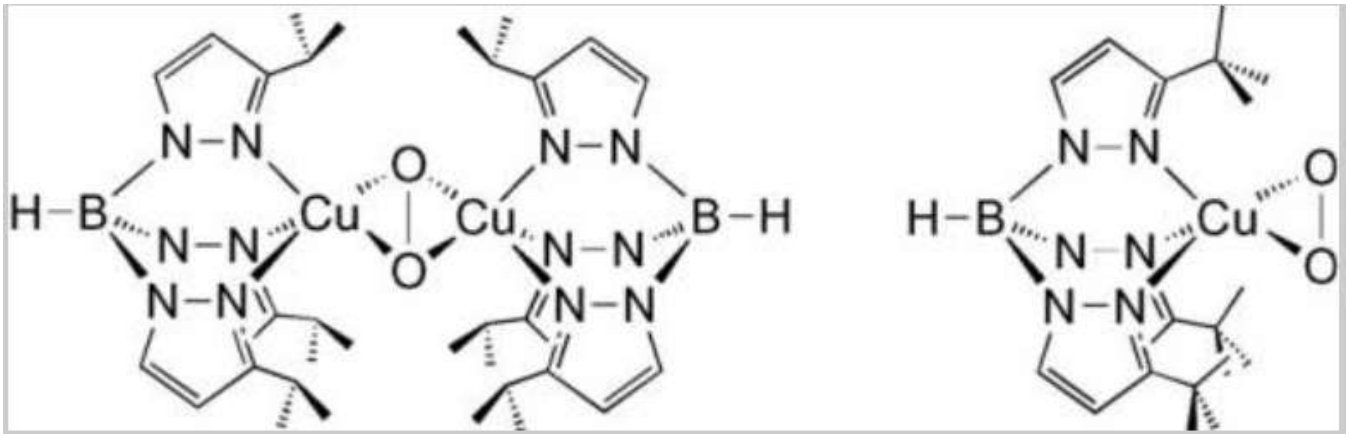

Fig. 1 - Kitajima's [TpR]Cuperoxo (left) and superoxo (right) complexes.

2. Ligand design and synthesis

The poly(thioether)borate ligands were introduced by this laboratory fifteen years ago to fill a perceived void in the types of tripodal ligands available for a variety of coordination and bioinorganic chemistry pursuits [12]. Specifically, we sought a monoanionic tripodal ligand containing highly polarizable donor groups, e.g. thioether sulfurs, reasoning that the latter attribute would afford access to lower valent metal complexes, e.g. nickel(I). We were certainly inspired by the utility Trofimenko'sTp ligands in a broad range of synthetic applications. In particular, at the time our work commenced Trofimenko had already introduced his second-generation ligands [14], those with larger substituents on the pyrazole, that proved effective in supporting lower coordinate metal complexes of the form, $[Tp^R]MX$. We reasoned that substitution on the thioether sulfur of poly(thioether)borates could have similar steric and electronic impact on the ligand derivatives. Indeed, given the substituent of the poly(thioether)borate ligand is attached directly to the metal donor atom, their influence should in principle be more pronounced than those of the $[Tp^R]$ ligands. Analogy with 1,4,7-trithiacyclononane (ttcn), a neutral tris(thioether) ligand is also relevant [15]. The coordination chemistry of ttcn is dominated by coordinatively saturated complexes of the form $(ttcn)_2M$ due to the lack of steric bulk around the donor atoms. The further development of ttcn derivatives entails modifications of the carbon backbone of the ligand and synthetic approaches to such derivatives require potentially dangerous synthetic intermediates, i.e. mustard gas analogs. Alternatively, neutral analogs of the Tt in which the boron is replaced with silicon have been shown to be labile, dissociating in coordinating solvents [16], highlighting the importance of the anionic charge of the borate in stabilizing chelation to charged metal ions.

While the initial ligand introduced was tetrakis((methylthio)methyl)borate (termed (RTt)), we quickly focused attention on tris(thioether)borates in which the fourth boron substituent is a phenyl group [17]. It should be noted that while the [Tp] (and [Bp]) ligands contain the B–H linkage, similar substitution in the poly(thioether)borates leads to derivatives, which are highly hydridic and consequently sensitive to moisture. This property is not surprising given the substitution pattern at boron of a hydride and three alkyl groups is analogous to the

'super hydride' reagent, $LiBEt_3H$. The phenyltris(thioether)borate ligands are prepared conveniently following the two-step protocol outlined in Scheme 1 [18]. The first step is deprotonation of a methyl sulfide by BuLi/TMEDA, followed by quenching of the resulting organolithium, $LiCH_2SR$, with 1/3 equivalent of $PhBCl_2$. The ligand salts are isolated as white air-stable solids, with the choice of counter ion dependent on the identity of the thioether. For example, we found it convenient to work with NBu_4^+ salts of [PhTt], whereas the Tl^+ salts of [$PhTt^{tBu}$] and [$PhTt^{Ad}$] are commonly employed. This strategy has been utilized to prepare bidentate ligands, [Ph_2Bt^R] [19,20], although the coordination chemistry of these ligands is less extensively developed providing an avenue for future development. Replacement of $PhBCl_2$ with $Fc\text{-}BBr_2$ allows for the synthesis of tris(thioether)borates containing the redox active ferrocenyl moiety, [FcTt] [21].

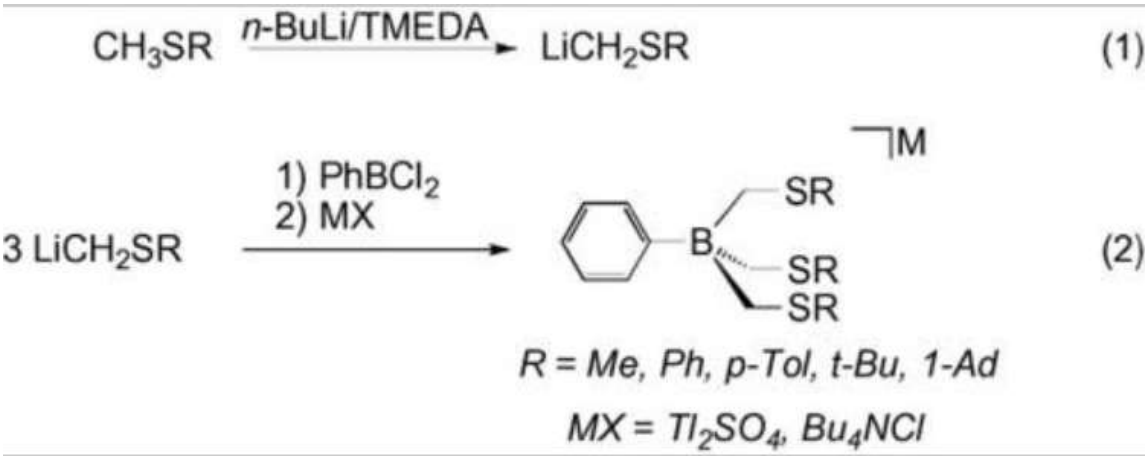

Scheme 1 - Ligand synthesis.

Modifying the synthetic protocol allows for the preparation of hybrid ligands containing both thioether and pyrazole donor groups. Tridentate ligands containing two thioethers and one pyrazole and bidentate ligands with one thioether and one pyrazolyl donor have been synthesized (Fig. 2) [22]. The one thioether, two pyrazole hybrid ligand that completes the series, [S_3], [S_2N], [SN_2], [N_3] has recently been reported [23]. The mixed donor ligands were prepared in one pot by sequential addition of $LiCH_2SR$ followed by lithium pyrazolylate [24]. With R = Me, the ligands were isolated as their Bu_4N^+ salts, whereas when R = *t*-Bu, we found it convenient to isolate the free acid of the ligand following aqueous work-up [25]. Given the opportunity to vary both the thioether and pyrazolyl ring substituents, a large number of hybrid ligand derivatives are possible. To date, we have focused on those ligands containing either methyl or *tert*-butyl thioether substituents and the parent or 3-*tert*-butyl pyrazoles.

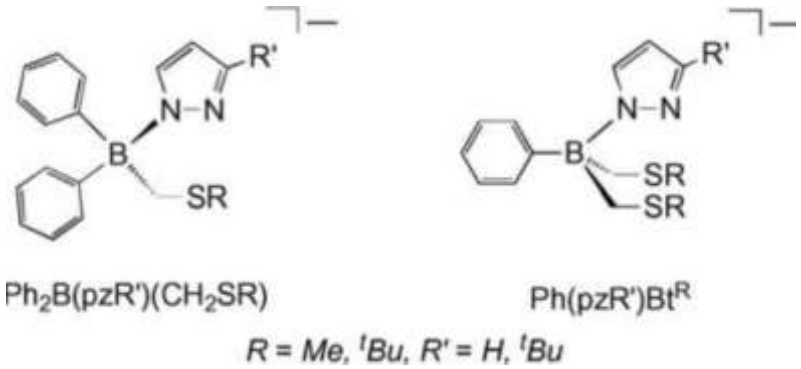

$Ph_2B(pzR')(CH_2SR)$ $Ph(pzR')Bt^R$

R = Me, ^{t}Bu, R' = H, ^{t}Bu

Fig. 2 - [SN] and [S2N] borate ligands.

3. Aspects of coordination chemistry

The ligand [PhTt] forms six-coordinate $[PhTt]_2M$ complexes with Fe(II), Co(II), Ni(II), Zn(II) and Cd(II) (Fig. 3) [17,26]. The corresponding palladium complex, $[PhTt]_2Pd$ is square planar [26]. The ligand field strength is moderate, as quantified below, such that $[PhTt]_2Fe$ exhibits spin-crossover behavior between the $^1A_{1g}$ and $^5T_{2g}$ states, whereas $[PhTt]_2Co$ is a low-spin complex. The latter exhibits the expected Jahn Teller distortion as indicated by an axial elongation in its structure as determined by X-ray diffraction and an axial EPR spectrum at 77 K [17]. Quantitative analysis of the electronic absorption spectrum of $[PhTt]_2Fe$ yields a ligand field splitting parameter of D_q = 1763 cm^{-1} (B = 420 cm^{-1}), which is ~100 cm^{-1}less than that of 1,4,7-triazacyclononane (tacn) and ~300 cm^{-1} weaker than ttcn. We have also compared the electronic donor aptitudes of tetrakis((methylthio)methyl)borate and tetrakis((phenylthio)methyl)borate via analysis of their $Mo(CO)_3$ adducts [12,27]. As shown in Table 1, the ν_{CO} stretching frequencies of $[(RTt)Mo(CO)_3]^-$ are the same energy as found for $[CpMo(CO)_3]^-$, indicating donors of comparable strength, whereas $[pzTp]^-$ is a stronger donor. Expectedly, replacement of the methyl thioether groups with the electron-withdrawing phenyl thioether shifts the ν_{CO} values to slightly higher energy.

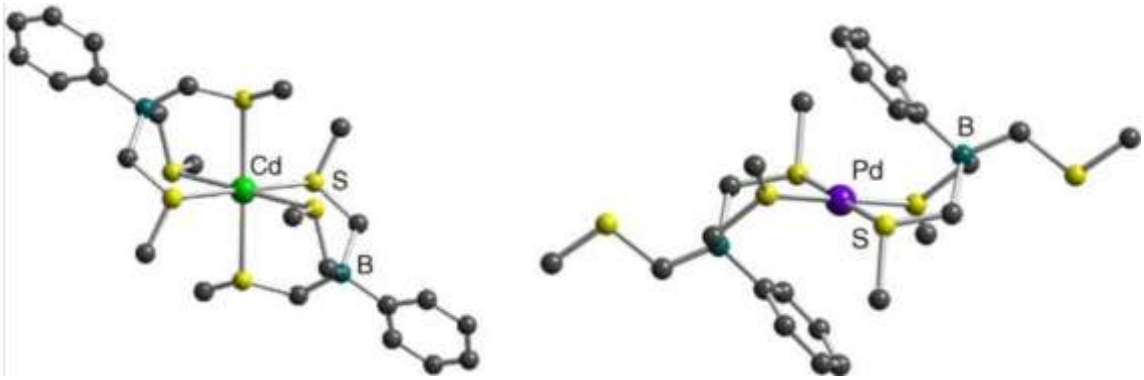

Fig. 3 - Structures of [PhTt]2Cd and [PhTt]2Pd.

Table 1

Comparative infrared data, ν_{CO} values, for $LMo(CO)_3$ derivatives.

	ν_{CO} (cm–1), A1, E
$(ttcn)Mo(CO)_3$ [28]	1925, 1815
$[Et_4N][(pzTp)Mo(CO)_3]$ [29]	1890, 1750
$Na[CpMo(CO)_3]$ [30]	1896, 1786, 1764
$[Bu_4N][(RTt)Mo(CO)_3]$ [12]	1899, 1784
$[Bu_4N][(R'Tt^{Ph})Mo(CO)_3]$ [27]	1910, 1785

A more comprehensive comparison of the electron–donor aptitude of tridentate monoanionic ligands is available in the series of LNi(NO) derivatives, in which the $^{\nu}$NO values of the linear nitrosyl ligand reports on the electron density at the nickel ion (Table 2). The value for $[PhTt^{tBu}]Ni(NO)$ is essentially identical to those of Cp*Ni(NO) and [Tp*]Ni(NO) indicating similar donor abilities of the tridentate ligands. Carbene and phosphine-derived borate ligands are significantly more electron rich, with $^{\nu}$NOvalues *ca*. 50–80 cm^{-1}lower in energy than the thioether borates.

Table 2

Comparative infrared data, $^{\nu}$NOvalues, for LNi(NO) derivatives

Comparative infrared data, $^{\nu}$NOvalues, for LNi(NO) derivatives.

	ν_{NO} (cm–1)
$[PhTt^{tBu}]Ni(NO)$ [31]	1785
CpNi(NO) [32]	1839
Cp*Ni(NO) [33]	1787
[Tp*]Ni(NO) [34]	1786
$[Tse^{Mes}]Ni(NO)$ [34]	1763, 1752
$[Tm^{tBu}]Ni(NO)$ [35]	1741
$[PhBP_3]Ni(NO)$ [36]	1737
$[HBIm^{tBu}]Ni(NO)$ [37]	1703

Abbreviations: Cp* = pentamethylcyclopentadienyl

[Tp*] = hydridotris(3,5-dimethyl-pyrazolyl)borate

$[Tse^{Mes}]$ = hydridotris(2-seleno-1-mesitylimidazolyl)borate

$[Tm^{tBu}]$ = hydridotris(mercapto-*tert*-butylimidazolyl)borate

$[HBIm^{tBu}]$ = hydrido(*tert*-butylimidazolyl)borate.

$[PhTt]_2M$ (M = Fe, Co, Ni) display rich electrochemical behavior in the cathodic direction [17]. $[PhTt]_2Fe$ undergoes a quasi-reversible reduction at a potential 90 mV above that of the Fc^+/Fc couple (unless noted otherwise, all potentials herein are referenced against this standard). $[PhTt]_2Co$ exhibits two cathodic events, a reversible couple at −530 mV and an irreversible reduction below −1.0 V. Both processes are proposed to be metal-based reductions with the reversible wave assigned to the Co(III/II) reduction based on chronoamperometry experiments. $[PhTt]_2Ni$ displayed two reductions below −1.0 V. Despite the rich cathodic electrochemistry, efforts to isolate and fully characterize the products of chemical reduction of these complexes were unsuccessful. However, as detailed later in this review, a change of ligand to $[PhTt^{tBu}]$ yielded lower coordination number complexes, i.e. $[PhTt^{tBu}]MX$, that afforded entry into a range of stable monovalent complexes. Alternatively, square planar $[Ph_2Bt]_2Ni$, which undergoes a quasi-reversible reduction at −1051 mV, is chemically reduced to a yellow nickel(I) complex, which displays a rhombic EPR signal, g = 2.27, 2.11 and 2.03 [19].

Efforts to prepare $[PhTt]_2Cu$ via similar ligand exchange reactions invariably led to bleaching of the solutions, an indication of metal reduction [38]. Indeed, we have been successful in preparing a wide range of copper(I) derivatives supported by the tris(thioether)borate ligands using copper(I) synthons [39]. In the absence of a fourth ligand, oligomeric and polymeric structures predominate. For example, $[(PhTt)Cu]_4$and $[(Ph_2Bt)Cu]_4$ exist in the solid state and in solution (non-coordinating solvents) as a tetramers with terminal and bridging thioethers (Fig. 4) [38,39]. Alternatively, $[PhTt^{Ph}]Cu$ and $[PhTt^{pTol}]Cu$ form extended chain solid state structures lacking bridging thioether ligands because the larger sulfur substituents preclude bridge formation [40]. These higher order structures are ruptured by donor ligands including phosphines, pyridine, thiolates, acetonitrile and CO yielding monomeric complexes, $[PhTt^{R}]Cu(L)$, or in the case of the bidentate ligands, $[Ph_2Bt^{R}]Cu(L)_2$ [39]. We have also used $[PhTt^{tBu}]Cu(NCCH_3)$ as a synthon in the preparation of CuNi bimetallic complexes (Fig. 5), as models for the inactive copper form of the A cluster in the enzyme acetyl coenzyme A synthase (ACS) [41]. In these derivatives two thiolates bridge the metal ions with the tetrahedral copper ligation completed by κ^2-$[PhTt^{tBu}]$. Carbonylation results in bridge rupture and formation of $[PhTt^{tBu}]Cu(CO)$. In general, the poly(thioether)borate ligands shift the Cu(II/I) redox potential so as to make the higher oxidation state inaccessible. Thus, the copper(I) complexes are stable to O_2, standing in stark contrast to the rich Cu(I)-dioxygen chemistry available to complexes containing polydentate nitrogen ligands [42].

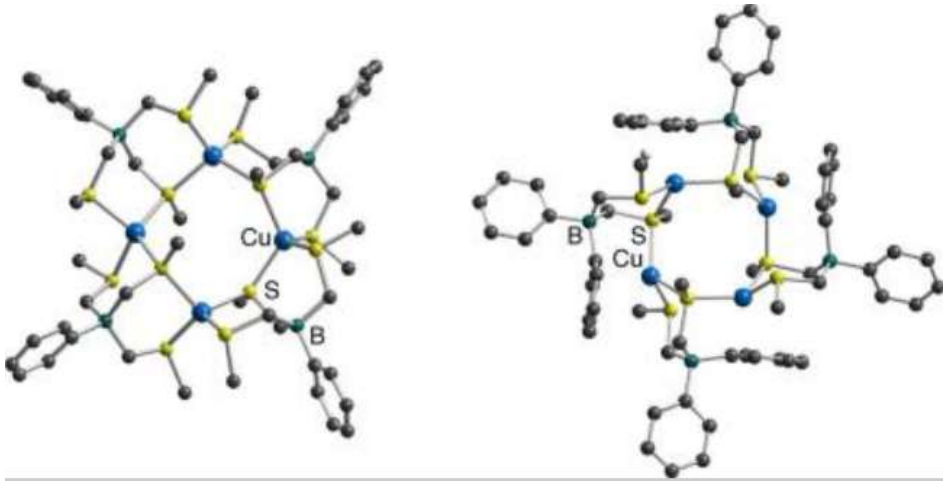

Fig. 4 - $[(PhTt)Cu]_4$ (left) and $[(Ph_2Bt)Cu]_4$ (right).

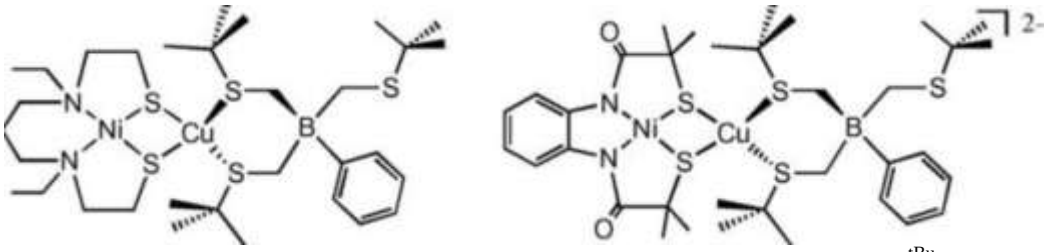

Fig. 5 - Thiolate-bridged nickel–copper complexes, $(Et_2N_2S_2)NiCu[PhTt^{tBu}]$ and $[(phmi)NiCu(PhTt^{tBu})]^-$.

In 1998, we reported $[PhTt^{tBu}]$ [31], a ligand with large *tert*-butyl thioether substituents that would serve to promote formation of $[PhTt^{tBu}]MX$ complexes, species that would be inherently more reactive than their $[PhTt]_2M$ brethren by virtue of the former's coordinative and electronic unsaturation. Complexes of Fe [43], Co [31], Ni [31], Zn [24], Cu [39], and Cd [24] have been prepared and fully characterized. While the derivatives of Fe, Co and Ni are paramagnetic, favorable electronic relaxation characteristics result in clear and informative paramagnetically dispersed ^1H NMR signals. Whereas in the initial report [31] we described $[PhTt^{tBu}]$ as a tetrahedral enforcing ligand, the ensuing decade has shown that numerous 5-coordinate complexes with this ligand are available, e.g. $[PhTt^{tBu}]Ni(NO_3)$ [44], $[(PhTt^{tBu})Cd]_2(\mu\text{-}Cl)_2$[24] and $[PhTt^{tBu}]Co(CO)_2$ [45]. Nonetheless, $[PhTt^{tBu}]$ has permitted us to explore a wide range of coordination, bioinorganic and organometallic pursuits. Key findings in these areas are summarized later in this review.

Whereas addition of one equivalent of $[PhTt^{tBu}]Tl$ to $NiCl_2$ or $Ni(NO_3)_2$ yields $[PhTt^{tBu}]NiX$, reactions performed in a 2 ligand:1 NiX_2 stoichiometry result in formation of the unexpected thianickelacycle (Scheme 2). This square planar, diamagnetic complex contains the $[PhTt^{tBu}]$ ligand coordinated in the κ^2-fashion and a η^2-CH_2S^tBu ligand derived from B–C bond rupture of a second $[PhTt^{tBu}]$ [46]. A similar organonickel complex $[Ph_2Bt^{tBu}]Ni(CH_2S^tBu)$, was produced when using the bidentate borate ligand, $[Ph_2Bt^{tBu}]$ [20]. In contrast, the smaller ligand $[Ph_2Bt]$ forms the expected square planar complex, $[Ph_2Bt]_2Ni$ [19]. It is clear that the steric requirements of the tert-butyl groups preclude formation of the $[PhTt^{tBu}]_2Ni$ species, opening a path for alkylation to the more stable thianickelacycles that are

thermodynamic sinks in a number of transformations. For example, attempted alkylation or reduction of [PhTt^{tBu}]NiCl in the absence of a suitable trapping ligand yields [PhTt^{tBu}]Ni(CH$_2$S^{t}Bu) [46]. We have observed formation of analogous metallacycles in cobalt chemistry [47], although we have not explored these to the depth of the nickel complexes.

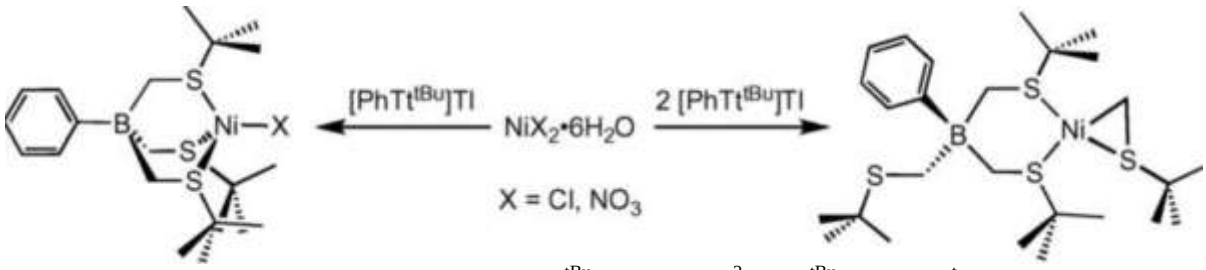

Scheme 2 - Synthesis of [PhTt^{tBu}]NiX and [κ^2-PhTt^{tBu}]Ni(CH$_2$S^{t}Bu).

3.1. Mixed donor [S$_2$N] and [SN] borate complexes

The least sterically hindered [S$_2$N] ligand, [Ph(pz)Bt] forms octahedral complexes with Fe, Co and Ni (Fig. 6) [22]. Structural and spectroscopic data revealed formation of the *cis* isomers exclusively, which place the nitrogen ligands *trans* to thioethers. The ligand field strength of [Ph(pz)Bt] is somewhat less than that of the tris(thioether) [PhTt] based on the observation that [Ph(pz)Bt]$_2$Co is high-spin whereas, [PhTt]$_2$Co is low-spin [17]. Both of the analogous iron complexes display spin-crossover behavior.

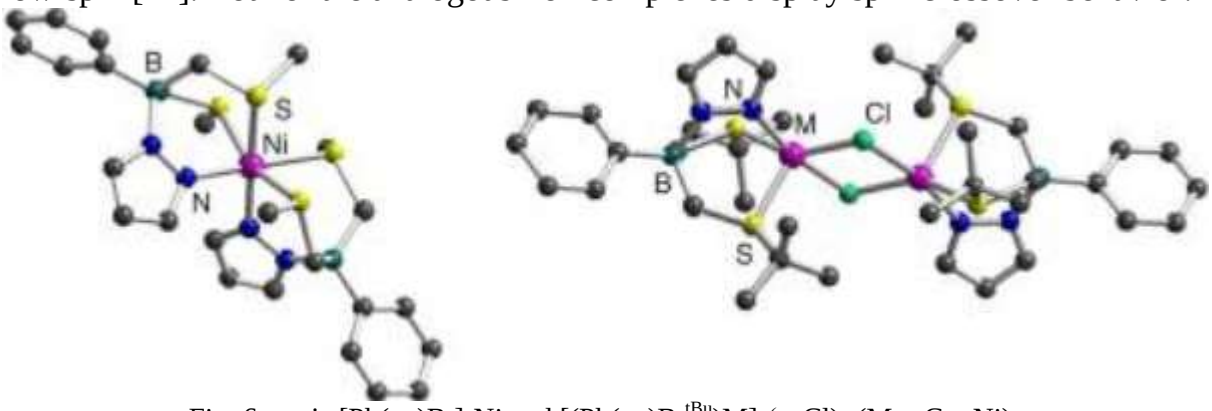

Fig. 6 - *cis*-[Ph(pz)Bt]$_2$Ni and [(Ph(pz)Bt^{tBu})M]$_2$(μ-Cl)$_2$ (M = Co, Ni).

The larger [Ph(pz)Bt^{tBu}] affords access to a range of metal complexes, many of the LMX form. Representative examples include [Ph(pz)Bt^{tBu}]ZnBr [24], [(Ph(pz)Bt^{tBu})Co]$_2$(μ-Cl)$_2$, [(Ph(pz)Bt^{tBu})Ni]$_2$(μ-Cl)$_2$ and [Ph(pz)Bt^{tBu}]Ni(acac) [48]. The chloride-bridged dimers (Fig. 6), reside on crystallographic inversion centers rendering the square pyramidal sites equivalent. Substituting Cd for Zn resulted in isolation of the tetrahedral 2:1 complex, [Ph(pz)Bt^{tBu}]$_2$Cd, with a N$_2$S$_2$ coordination sphere. Each borate ligand coordinates via one thioether and the pyrazole donor. This complex was formed regardless of reaction stoichiometry, i.e. reactions performed in 1:1 and 2:1 ligand:metal ratios yielded the same product [48]. Metallation of $CoCl_2$ gives a variety of products dependent upon reaction conditions (Scheme 3) [48]. Addition of the free acid ligand to $CoCl_2$ in THF or acetone cleanly yields tetrahedral [Ph(pzH)Bt^{tBu}]$CoCl_2$. In this complex, the ligand remains protonated at the pyrazole leaving the two thioethers to coordinate to Co. In the X-ray structures, the

solvent (THF or acetone) is H-bonded to the ligand proton. Reacting [Ph(pz)Bt^{tBu}]K with.

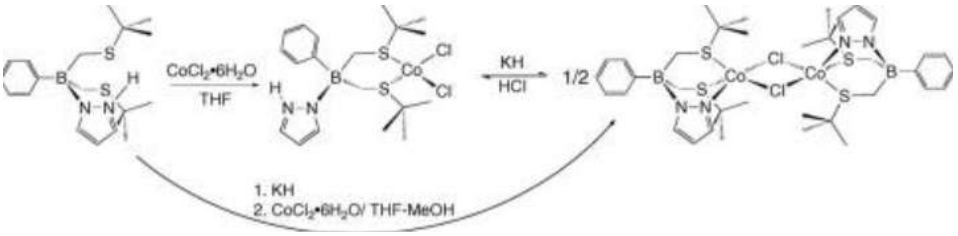

Scheme 3

$CoCl_2$ in THF/acetonitrile generates an equimolar mixture of [(Ph(pz)Bt^{tBu})Co]$_2$(μ-Cl)$_2$ and [Ph(pzH)Bt^{tBu}]$CoCl_2$·THF [48]. The two products were separated based on their differential solubility. Surprisingly, when the latter reaction was conducted in THF/MeOH yet another product was obtained in high yield. [Ph(pz)Bt^{tBu}]$_2$Co features tetrahedral ligation with each borate ligand coordinated via one thioether and pyrazole donor. [(Ph(pz)Bt^{tBu})Co]$_2$(μ-Cl)$_2$ and [Ph(pzH)Bt^{tBu}]$CoCl_2$·THF are related by acid-base chemistry. Addition of KH to [Ph(pzH)Bt^{tBu}]$CoCl_2$·THF yields the chloride-bridged dimer (Scheme 3). The reaction can be reversed by addition of a concentrated THF solution of HCl.

We have utilized the ligand [Ph(pz^{tBu})Bt^{tBu}], containing *tert*-butyl substituents on the thioethers and the 3-pyrazole position, to prepare monomeric Zn and Cd complexes [25] as models for the actives sites of methionine synthase, a family of zinc proteins, as described in the following section.

Go to:

4. Analogs of monomeric metal–thiolate sites in proteins

4.1. Zinc thiolates

[PhTt^{tBu}] and [Ph(pz^{tBu})Bt^{tBu}] provide the appropriate donors sets to model aspects of the structure and function of the family of mononuclear zinc proteins that activate thiol cofactors [49], and thus, have been used for this purpose. Representative members include the two forms of methionine synthase that are responsible for the final step in the biosynthesis of the amino acid methionine. Nature has evolved two pathways, one cobalamin-dependent (Met H) and the other independent (Met E) of the B_{12} cofactor, which entail homocysteine methylation by methyl tetrahydrofo-late. The four coordinate zinc sites (Fig. 7) contain three protein residues and a fourth labile ligand site for homocysteine binding. The metal ion is proposed to bind the thiolate substrate rendering it sufficiently nucleophilic for attack by carbon electrophiles [49]. Using synthetic chemistry, a series of mononuclear zinc thiolate complex models [25] were prepared with the [PhTt^{tBu}] and [Ph(pz^{tBu})Bt^{tBu}] borate ligands providing the ancillary donor arrays found in Met H and Met E, respectively (Fig. 7). [Tp^R], [Tm^R] and hybrid donor based synthetic analogs have been described by Vahrenkamp and co-workers [50], Parkin and co-workers [51] and Carrano and co-workers [52]. The thioether donors have a reduced proclivity to bridge between and among metals, ensuring formation of monomeric complexes while at the same time, modeling metal–sulfur interactions. Metal–cysteine bonds in biology may be modified by hydrogen bonding [53] and local environment dielectrics that serve to reduce the nucleophilic character of the thiolate and alter redox potentials of redox active metal ions. Thus, at least in these contexts, thioether donors may accurately model these characteristics.

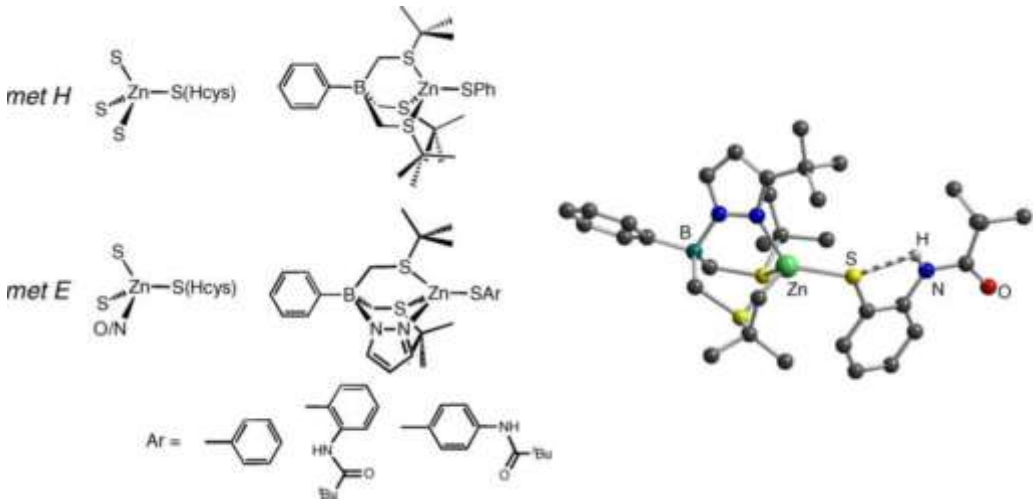

Fig. 7 - Active site coordination environments and associated model complexes for the homocysteine (Hcys) ligated states of the zinc sites in the methionine synthases and structure of synthetic complex containing an internal S· · ·H–N bond (right).

Reaction of the zinc thiolate complexes with alkyl halides led cleanly to the corresponding thioether and zinc halide [25]. In toluene, the reactions exhibits second-order kinetics with activation parameters consistent with a S_N2 attack of the zinc thiolate on the carbon of the alkyl halide. The transformation serves as a reactivity model for the thiol-activating proteins and in particular revealed the influence of an intramolecular hydrogen-bond on modulating the zinc thiolate nucleophilicity [54]. The zinc thio-late complex containing an *ortho*-pivalyl amido substituent that provides a H-bond donor to the thiolate is alkylated 20× slower than the complex lacking this *ortho* substituent. Further, the H-bonding shows an inverse isotope effect, k_H/k_D = 0.33 at 60 °C [25]. The slower reaction of the deuterium analog was rationalized based on equilibrium differences in zero point energies between the H/D-bonded and non-H/D-bonded zinc thiolates. A related study by Parkin on similar zinc thiolate complexes uncovered a normal kie, k_H/k_D = 1.16 at 0 °C, consistent with thiolate dissociation preceding alkylation as supposed by DFT studies [51]. The same report provided DFT evidence predicting that alkylation of a zinc-bound thiolate would exhibit an inverse isotope effect, lending further support to our proposed mechanism.

4.2. High-spin nickel thiolates

Nickel–thiolate linkages are found in a number of metalloproteins with diverse functions including superoxide dismutase [55], hydrogenases [56], methyl coenzyme M reductase [57], and acetyl coenzyme A synthase [58]. A common feature among these proteins is requisite redox activity of the nickel ion. Despite the prevalence of nickel–cysteine bonding in biology, synthetic complexes containing a single nickel–thiolate linkage, particularly in high-spin states, are uncommon [44,59] primarily due to the propensity with which thiolates bridge between and among metal ions favoring higher order structures [60]. To examine the characteristics of a single nickel–thiolate bond in high-spin nickel(II) complexes, the series [$PhTt^{tBu}$]Ni(SR) (R = C_6H_5, C_6F_5, Ph_3C) was prepared and fully characterized (Scheme 4) [44]. Reaction of [$PhTt^{tBu}$]Ni(NO_3) with the corresponding thiol and triethyl amine affords dark violet to purple solutions from which the nickel thiolate complexes were crystallized. The four-coordinate structures approximate a trigonal pyramid with a thioether occupying

the apical position. This geometry enhances the π-orbital overlap involved in the LMCT transitions. The more electron-withdrawing thiolate substituents move the CT transition to higher energy, presumably due to stabilization of the sulfur $p_\pi$orbital energy. The nickel thiolates complexes are subject to quasi-reversible electrochemical reduction to nickel(I) suggesting that the reduced forms may be accessible via chemical synthesis. The reduction potentials exhibit a similar trend as a function of thiolate substituent with the most electron-withdrawing group showing the most accessible reduction potential.

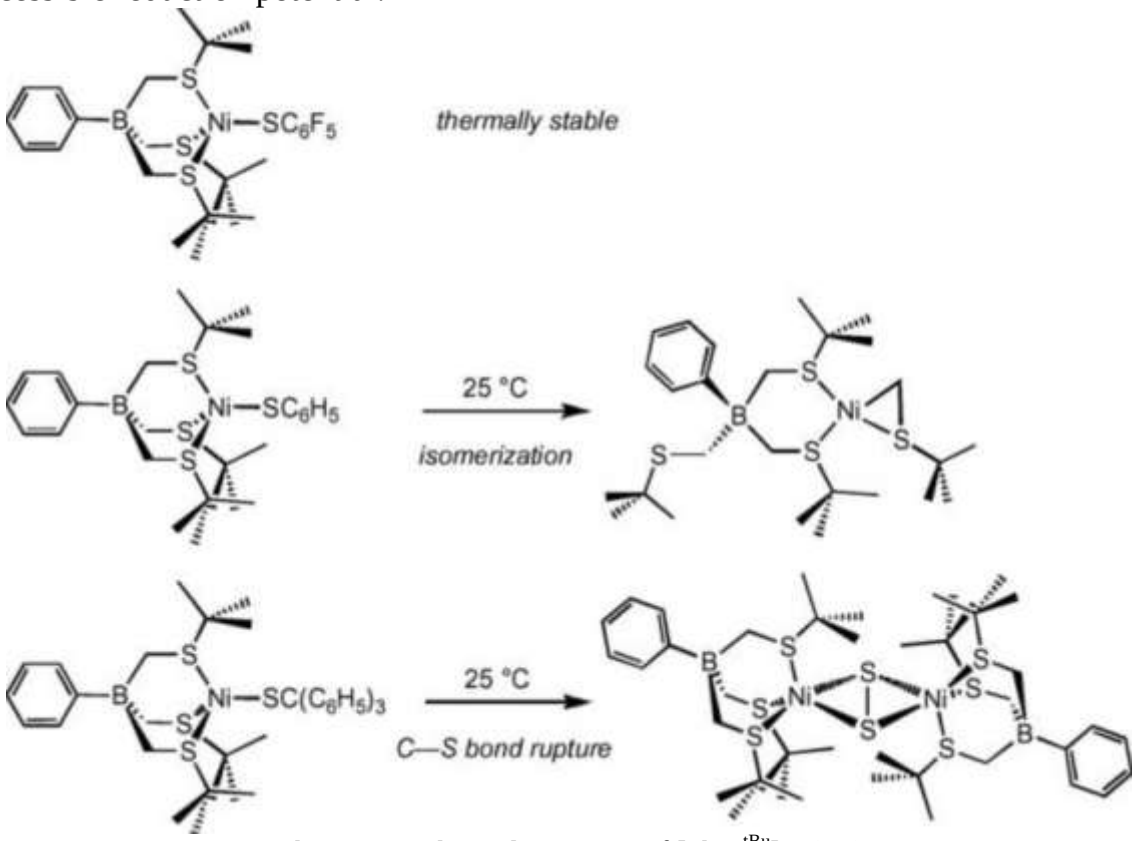

Scheme 4 - Thermal reactivity of [PhTt^{tBu}]Ni(SR).

The nickel thiolate complexes exhibit contrasting thermal stabilities. While [PhTt^{tBu}]Ni(SC_6F_5) is stable up to its melting point, [PhTt^{tBu}]Ni($SCPh_3$) and [PhTt^{tBu}]Ni(SPh) undergo room temperature reactions. [PhTt^{tBu}]Ni($SCPh_3$) converts to [(PhTt^{tBu})Ni]$_2$(μ-S_2) [61] via C–S bond rupture, whereas [PhTt^{tBu}]Ni(SPh) isomerizes [44] to the square planar thiametallacycle in which the B–CH_2S^tBu and Ni–SPh groups exchange (Scheme 4). The latter rearrangement was proposed to proceed via intramolecular nucleophilic attack of the phenylthiolate on boron. Consistent with this hypothesis, [PhTt^{tBu}]Ni(SC_6F_5) containing a less nucleophilic thiolate does not undergo isomerization, even at elevated temperature.

5. Organo-cobalt and organo-iron complexes

Emphasis in recent years has been placed on the synthesis of high-spin, low-coordinate and low electron count, i.e. less than 18 electron, organometallic complexes [62–65] because of their potential roles in a wide range of chemical transformations as well as their inherently novel geometric and electronic structures that are distinct from the plethora of low-spin, 18-electron count species. Leading examples include organometallic complexes supported by tridentate (Tp) [62,64,66] and bidentate (β-diketiminate) [65] donors as well as homoleptic complexes with

exceedingly large donors [67]. Our own efforts have concerned the synthesis of four-coordinate organometallic complexes of nickel, cobalt and iron supported by [PhTt^{tBu}]. The highly polarizable thioethers represent a rarely explored donor set for organometallic chemistry. These studies were initially motivated by the goal of preparing four-coordinate, high-spin organonickel complexes of relevance to purported intermediates in nickel biocatalysis; an objective that remains to be achieved.

Diorganomagnesium reagents R_2Mg (R = Me, Et, Ph, Bn) react cleanly with [PhTt^{tBu}]CoCl and [(PhTt^{tBu})Fe]$_2$(μ-Cl)$_2$ yielding the thermally stable organometallic derivatives. The R = Me and Bn derivatives of Fe and Co were characterized by X-ray diffraction analyses [68,69]; the Bn derivatives feature η^1-benzyl ligation. The complexes exhibit magnetic moments consistent with high-spin states, S = 3/2 for Co and S = 2 for Fe. Low field Mössbauer spectroscopy performed on [PhTt^{tBu}]Fe(Me) revealing an isomer shift of δ = 0.60(3) mm/s and a quadrupole splitting of ΔE_Q = 0.00(1) mm/s, values in good agreement with DFT-calculated parameters for the high-spin ferrous complex [70]. Further, this complex displays unusual magnetic characteristics, namely, a negative and large zero-field splitting ($D = -33(3)\text{cm}^{-1}$) and a large uniaxial orbital hyperfine component [71] (coincident with the Fe–C vector). The η^3-allyl complexes of Co and Ni have been synthesized similarly and are five- and four-coordinate respectively, by virtue of κ^3- and κ^2-[PhTt^{tBu}] ligation [68]. In contrast to square planar [κ^2-PhTt^{tBu}]Ni(η^3-allyl), [Tp^{iPr2}]Ni(η^3-allyl) [63] is square pyramidal with one pyrazole occupying an apical site.

Despite their coordinative and electronic unsaturation, the high-spin cobalt and iron complexes are thermally stable. For example, the ethyl derivatives do not undergo β-hydrogen elimination, it has been argued because the metal orbital required for hydrogen migration is partially filled, a consequence of the high-spin state [63]. Nonetheless, other transformations that require vacant metal-based orbitals proceed rapidly at ambient temperature and pressure. For example, [PhBP$^{iPr}_3$]Fe(R) complexes are susceptible to rapid hydrogenolysis with H_2 [72]. The organo-iron [69] and organo-cobalt [68] complexes herein undergo facile reaction with CO yielding several different products depending upon the identity of the alkyl/aryl group (Scheme 5). Carbonylation of [PhTt^{tBu}]Co(R), R = Me, Et, Ph, results in a rapid color change from green to red signaling formation of low-spin [PhTt^{tBu}]Co(CO)(C(O)R). Alternatively, [PhTt^{tBu}]Co(Bn) and [PhTt^{tBu}]Co(η^3-allyl) are reduced to the monovalent [PhTt^{tBu}]Co(CO)$_2$ by CO. We have further found that this dicarbonyl adduct is in equilibrium with the high-spin monocarbonyl, [PhTt^{tBu}]Co(CO) [68]. For comparison, CO addition to [Tp^{tBu}]Co(Me) yielded [Tp^{tBu}]Co(CO) [64] and the smaller [Tp^{iPr2}]Co(R), R = allyl, *p*-methylbenzyl, converted to [Tp^{iPr2}]Co(CO)(C(O)R) [63]. Addition of CO to [PhTt^{tBu}]Fe(R), R = Me, Et, Ph, produces [PhTt^{tBu}]Fe(CO)$_2$(R) [69], analogs of the well knownFp-R. However, carbonylation of [PhTt^{tBu}]Fe(Bn) generates a mixture of [PhTt^{tBu}]Fe(CO)$_2$(Bn) and [PhTt^{tBu}]Fe(CO)$_2$, the latter a minor species resulting from Fe–Bnhomolysis. In contrast, carbonylation of [Tp^{iPr2}]Fe(R) produced 18-electron [Tp^{iPr2}]Fe(CO)$_2$(C(O)R) [63]. In sum, the [PhTt^{tBu}] Co and Fe complexes containing alkyl groups that yield stabilized radicals, e.g. Bn and allyl, undergo M–R homolysis followed by trapping of the monovalent metal fragment with excess CO. The ability of [PhTt^{tBu}] relative to [Tp^R] to favor formation of the lower valent complexes is a facet exploited to explore the synthesis and reactivity of

monovalent complexes of Fe, Co and Ni.

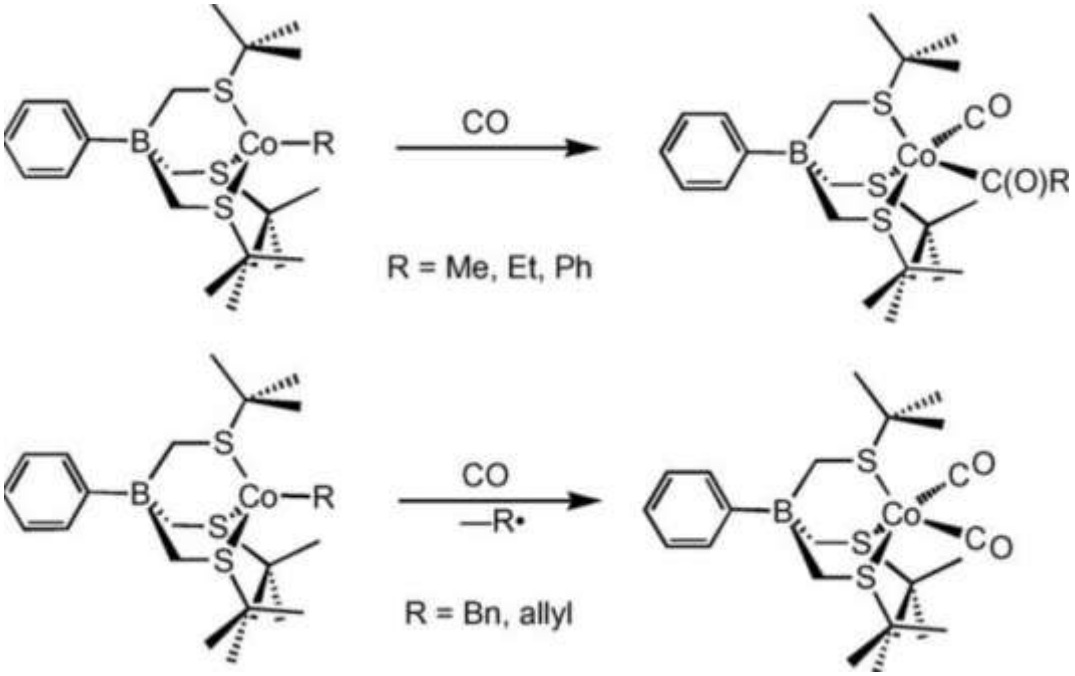

Scheme 5

6. Monovalent complexes of nickel, cobalt and iron

Entry into monovalent complexes supported by [PhTt^{tBu}] resulted from observations made during efforts to prepare high-spin organonickel complexes. Specifically, addition of Me_2Mg or MeLi to [PhTt^{tBu}]NiCl produced diamagnetic red-orange [κ^2-PhTt^{tBu}]Ni(CH_2S^tBu) in modest yield (Scheme 6) [46]. We hypothesized that if [PhTt^{tBu}]Ni(Me) was formed as an intermediate on the pathway to the thianickelacycle, it might be possible to intercept this intermediate via addition of suitable donor ligands that could stabilize a square planar adduct, i.e. [κ^2-PhTt^{tBu}]Ni(L)(Me). Thus, addition of MeLi to [PhTt^{tBu}]NiCl in the presence of CO [46], PMe_3 [46], PPh_3 [73] or CN^tBu [74], was conducted. The reaction yielded the nickel(I) adducts, [PhTt^{tBu}]Ni(L), as yellow crystalline materials (Scheme 6). Similarly, Na amalgam reduction of [PhTt^{tBu}]NiCl yields the same products in the absence and presence of trapping ligand. These observations led to the conclusion that Me_2Mg (or MeLi) effects reduction of [PhTt^{tBu}]NiCl via single electron transfer without intermediacy of [PhTt^{tBu}]Ni(Me). Indeed, following a survey of potential reductants, it was determined that MeLi afforded [PhTt^{tBu}]Ni(L) in the best yields. This strategy was extended to derivatives with the bulkier ligand, [PhTt^{Ad}], specifically [PhTt^{Ad}]Ni(L), where L = CO and PMe_3 [75]. As described in the next section, the [PhTt^{R}]Ni(L) complexes activate $O_2$and S_8 leading to isolable nickel chalcogenide species. The similarity of the energies of the ν_{CO} band in [PhTt^{tBu}]Ni(CO), 1999 cm^{-1} [46], and in the A_{red}–CO spectroscopic state of the A cluster in ACS, 1995 cm^{-1} [76], prompted detailed spectroscopic and computational studies of the synthetic complex [77].

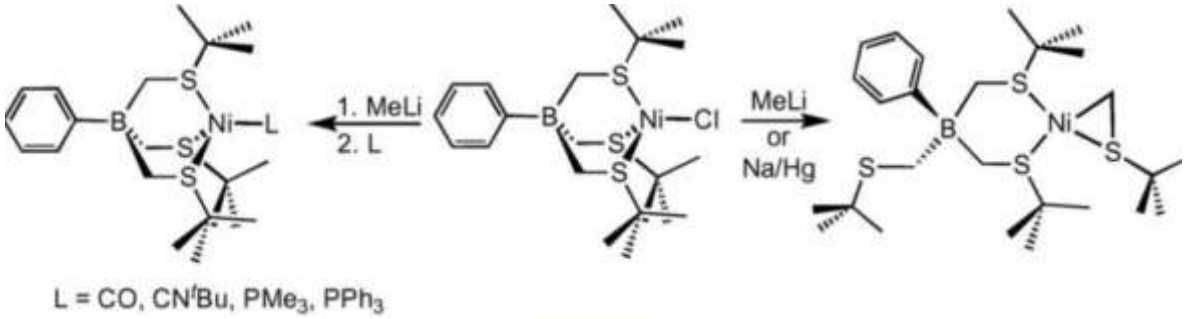

Scheme 6

Sodium amalgam reduction of ethereal solutions of [PhTt^{tBu}]CoCl in the presence of phosphines, phosphite or CN^{t}Bu effects the formation of the 16-electron cobalt(I) complexes, [PhTt^{tBu}]Co(L) [45]. Analysis of the molecular structures of the [PhTt^{tBu}]Co(L) complexes reveals that the L donor resides off the inherent three-fold axis to varying degrees, a phenomenon first noted and rationalized by Theopold via a Walsh diagram analysis that considers bending of the L off axis [78]. The most distorted structures, L = P(OPh)$_3$ and NC^{t}Bu, may be described as cis divacantoctahedra, a term used previously for [Tp^{Np}]Co(CO) [78]. For the six complexes examined, there was a clear correlation between the structural distortion and the electronic character of the phosphine or phosphite. Whereas, pure σ-donor ligands, e.g. PMe$_3$, show little distortion, π-acceptor ligands are located off-axis. For example, in [PhTt^{tBu}]Co(P(OPh)$_3$), the phosphite is 23.6° off-axis (Fig. 8).

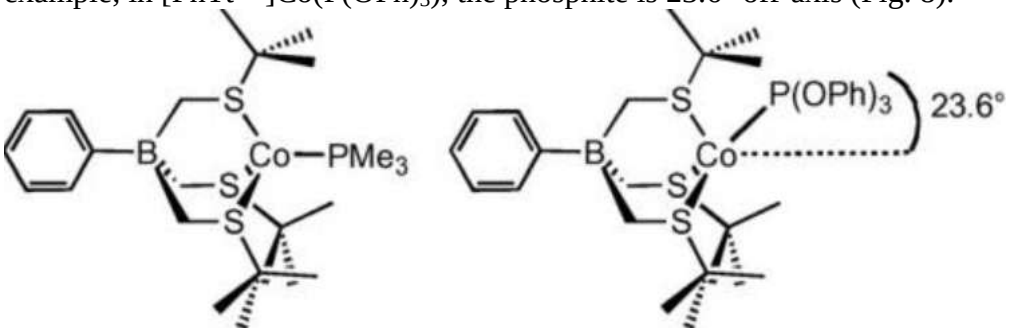

Fig. 8 - Structures of Co(I) complexes as a function of phosphine: σ-donor phosphines reside on the three-fold axis, whereas π-acceptor ligands lead to a distorted geometry.

The corresponding iron(I) phosphine complexes are prepared by KC_8 reduction of the dimer, {[(PhTt^{tBu})]Fe}$_2$(μ-Cl)$_2$, in the presence of PMe$_3$ or PEt$_3$ [43]. The phosphine ligands are located on the three-fold axis. High-spin [PhTt^{tBu}]Fe(PMe$_3$) exhibits an axial EPR signal with g = 4.26, 2.05 at 5K and E/D = 0. It's Möss-bauer parameters are δ = 0.76(3) mm/s and ΔE_Q = 1.88(3) mm/s, with the isomer shift greater than values reported for the limited set of iron(I) complexes interrogated by Mössbauer spectroscopy [43]. [PhTt^{tBu}]Fe(PMe$_3$) is a synthon for a number of derivatives accessible by replacement of the phosphine ligand (Scheme 7). Carbonylation leads to [PhTt^{tBu}]Fe(CO)$_2$, a low-spin square pyramidal iron(I) complex that is of relevance to reduced states of the diiron hydrogenases. The rhombic EPR signal, g = 2.13, 2.07, 2.00, is similar to that reported for the oxidized form of hydrogenase II, g = 2.078, 2.027, 1.99 [79]. Addition of diphenylacetylene to [PhTt^{tBu}]Fe(PMe$_3$) produces square pyramidal [PhTt^{tBu}]Fe(PhCCPh) [43], a high-spin complex with significant metallacyclopropene character resulting from π-donation from iron to the alkyne. Whereas, the ^{1}H NMR spectral data are similar to those of other ferrous [PhTt^{tBu}]Fe complexes, the isomer shift, δ = 0.62(3) mm/s and quadrupole coupling, ΔE_Q = 1.62(2) mm/s are not inconsistent with a high-spin iron(I) complex.

Addition of 1-adamantyl azide to [PhTt^{tBu}]Fe(PMe$_3$) yields the diadamantyltetraazadiene, rather than the anticipated adamantyl imide, [PhTt^{tBu}]Fe(NAd). Corresponding imides and

nitrides containing tris(phosphino)borate [80] and tris(carbene)borate [81] have been structurally characterized. The structure of [κ^2-PhTt^{tBu}]Fe(N_4Ad_2) features bidentate ligation of the borate ligand and a planar FeN_4 metallacyclic ring resulting in approximate tetrahedral stereochemistry at iron [43]. The metric parameters of the FeN_4unit, specifically similar N–N bond lengths, indicate the best resonance descriptor of the tetraazadiene is as a monoanion [82]. Thus, the molecule can be viewed as a high spin ferrous complex coordinated to two anionic ligands. A reasonable mechanism that yields [κ^2-PhTt^{tBu}]Fe(N_4Ad_2) entails initial group transfer generating an incipient adamantyl imide followed by 3 + 2 addition of a second adamantylazide [83]. Further support for this mechanism comes from Holland's recent report of AdN_3 addition to an imidoiron(II) adduct yielding a tetraazadiene adduct [83].

7. Dioxygen and sulfur reactions with monovalent nickel

Yellow [PhTt^R]Ni(CO), R = ^{t}Bu or Ad, reacts with O_2 at sub-ambient temperatures to generate distinct, thermally unstable intermediates that have been characterized by a wide range of spectroscopic and structural methods and further analyzed by DFT computations (Scheme 8). With the smaller *tert*-butyl thioether substituents, [PhTt^{tBu}]Ni(CO) is oxygenated to the bis-μ-oxo dinickel(III) species in which the O_2 undergoes a four electron reduction with concomitant O–O bond rupture [84]. The planar Ni_2O_2rhomb displays short Ni–O, 1.82 Å and Ni· · ·Ni, 2.83 Å separations deduced by extended X-ray absorption fine structure (EXAFS) measurements. Distinct spectroscopic features include an intense O → Ni CT transition at 565 nm and an oxygen isotope sensitive ν_{Ni-O} resonance Raman band at 590 cm^{-1}[85]. [(PhTt^{tBu})Ni]$_2$(μ-O)$_2$ is diamagnetic, a consequence of strong antiferromagnetic coupling between the nickel(III) sites. In contrast, oxygenation of [PhTt^{Ad}]Ni(CO) yielded the monomer [PhTt^{Ad}]Ni(O_2) featuring a side-on dioxygen ligand [86]. The adamantylthioether substituents serve to preclude bis-μ-oxo dimer formation under these conditions. Paramagnetic [PhTt^{Ad}]Ni(O_2) displays a rhombic EPR signal, g= 2.24, 2.19, 2.01, consistent with its doublet ground state. DFT-derived natural orbitals include a σ-bonding Ni-O_2 HOMO and a SOMO that is largely Ni d_z^2 in character. A nickel-centered unpaired electron is in agreement with EPR and DFT analyses. While a nickel(II)-superoxo description is in line with all of the spectroscopic and computational data, based on the DFT-derived O–O distance Tolman and co-workers have suggested [87] a more activated dioxygen adduct, i.e. a structure further along the superoxo-to-peroxo continuum.

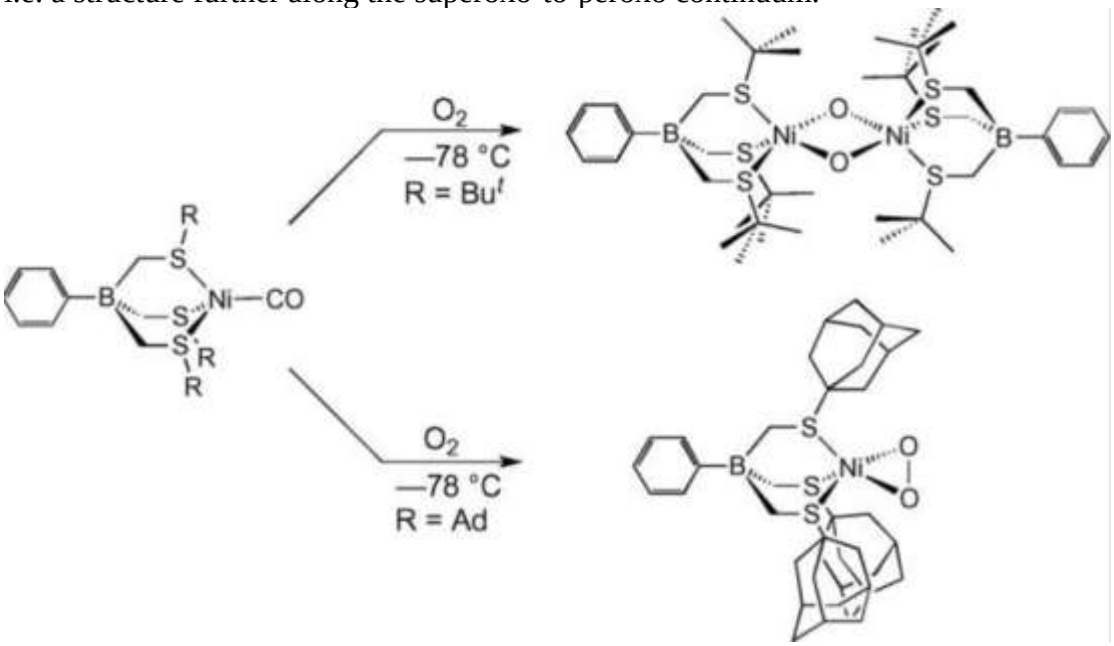

Scheme 8

The ability to intercept metastable nickel–oxygen adducts supported by the [$PhTt^R$] ligands derives, at least in part, from the heretofore lack of thioether sulfur oxidation. As is common for such reactive intermediates, we believe kinetically controlled ligand and/or solvent C–H activation represents the major decomposition pathway(s). Similar oxidative robustness towards ligand donor oxidation is found in the [Tp^R] ligands rendering them extremely popular scaffolds for metal-based dioxygen activation [6]. Conversely, [$PhBP_3$] and tris(carbene) ligands have been shown to be susceptible to phosphorus [36,88] and carbon [89] oxidation via insertion of [O] (or [NR]) into the metal–ligand bonds.

Formation of [$(PhTt^{tBu})Ni]_2(\mu\text{-}O)_2$ is proposed to proceed in a stepwise process with initial generation of a 1:1 adduct followed by subsequent dimerization. Optical and EPR spectral interrogation of the reaction showed evidence for generation of the 1:1 intermediate, [$PhTt^{tBu}$]Ni(O_2), the *tert*-butyl analog of well-characterized [$PhTt^{Ad}$]Ni(O_2). Further evidence in support of this mechanism is found in the reaction of [$PhTt^{Ad}$]Ni(O_2) with [$PhTt^{tBu}$]Ni(CO) that yielded the mixed-ligand bis-μ-oxo dinickel(III) complex [86]. The utility of metal–dioxygen complexes as synthons for new structures types is further exemplified by the reaction of the side-on peroxo-copper(III) complex, [iPr_2nacnac]Cu(O_2), with [$PhTt^{tBu}$]Ni(CO) [90]. The nickel(I) further activates the dioxygen moiety leading to a mixture of μ-peroxo and bis-μ-oxo mixed metal dimers of which the latter is the majority species.

[$PhTt^{tBu}$]Ni(CO) also activates S_8, although the transformation is rather slow, taking approximately one week to reach completion at room temperature [61]. For comparison, oxygenation of [$PhTt^{tBu}$]Ni(CO) occurs within hours at −78 °C [84]. The thermally stable product is also accessible via room temperature decomposition of [$PhTt^{tBu}$]Ni($SCPh_3$), a process entailing C–S bond cleavage [61,91]. The planar disulfidodinickel(II) core contains a $\mu\text{-}\eta^2\text{:}\eta^2\text{-}S_2$ ligand symmetrically located between the two nickel centers (Fig. 9). The S–S distance of 2.177 Å reflects a reasonably activated disulfide moiety. The ν_{S-S} vibrational mode at 446 cm^{-1} was assigned based on its energy and isotopic sensitivity. In samples prepared from $^{34}S_8$ the band moved to 437 cm^{-1}. In the dimer, strong antiferromagnetic coupling, $-2J$ = 952 cm^{-1}, results in a diamagnetic ground state. [$(PhTt^{tBu})Ni]_2(\mu\text{-}\eta^2\text{:}\eta^2\text{-}S_2)$ is distinct from its congener, [$(PhTt^{tBu})Ni]_2(\mu\text{-}O)_2$, in terms of formal metal oxidation state and the presence (disulfide) or absence (bis-μ-oxo) of a dichalcogenide bond. A combination of more extensive Ni dπ → O_2 σ* back-bonding and higher σ-donation of the oxo ligands serve to stabilize the dinickel(III) in [$(PhTt^{tBu})Ni]_2(\mu\text{-}O)_2$. [$(PhTt^{tBu})Ni]_2(\mu\text{-}\eta^2\text{:}\eta^2\text{-}S_2)$ may be considered as a model for the unprecedented $\mu\text{-}\eta^2\text{:}\eta^2$-peroxodinickel complexes [85] that may be intermediates along the pathway to bis-μ-oxo dinickel(III) formation.

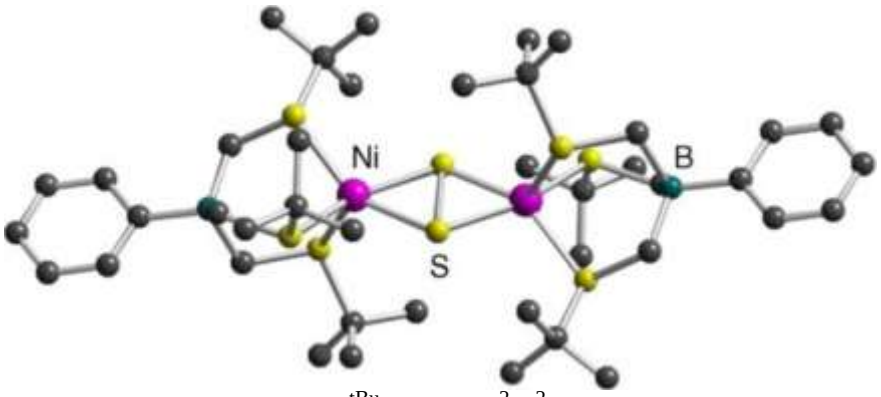

Fig. 9 - Structure of [$(PhTt^{tBu})Ni]_2(\mu\text{-}\eta^2\text{:}\eta^2\text{-}S_2)$.

8. Summary

The poly(thioether)borates have proven to be a new ligand type of some utility in a range of synthetic pursuits spanning objectives in coordination, organometallic and bioinorganic chemistry. The combination of the anionic charge afforded by the borate and the chelate effect of the polydentate ligands are characteristics that yield strong chelation. This strategy has vastly expanded the coordination chemistry of acyclic thioether donors, which are generally regarded as weak and often labile donors. Significantly, by varying the sulfur substituent, it is possible to tune the structure and reactivity of the attendant metal complex, sometimes in predictable ways, largely based on the steric requirements of the thioether. When the ligands are affixed to metal ions, they have proven to be robust, for example, even to sulfur oxidation in the presence of H_2O_2. We have encountered several examples of B–C bond cleavage and have tried to understand the pathways leading to such ligand degradation.

While the areas developed to date reflect the objectives of this laboratory, it seems clear that there are additional opportunities for future exploration. For example, the bis(thioether)borates, particularly derivatives with large substituents that would favor low coordinate complexes, can be viewed as 'softer' versions of the β-diketiminate ligands. Alternatively, the coordination chemistry of the heavier transition series metals has been little explored. The favorable match of the polarizable thioether donors and the heavier metals should yield robust complexes. In this context, the utility of the ligands to sequester metal ions from complex media could be considered. Our own interests continue to be directed toward small molecule activation as a strategy to access both new structure types and inherently reactive intermediates of utility in stoichiometric and ultimately, catalytic chemical transformations.

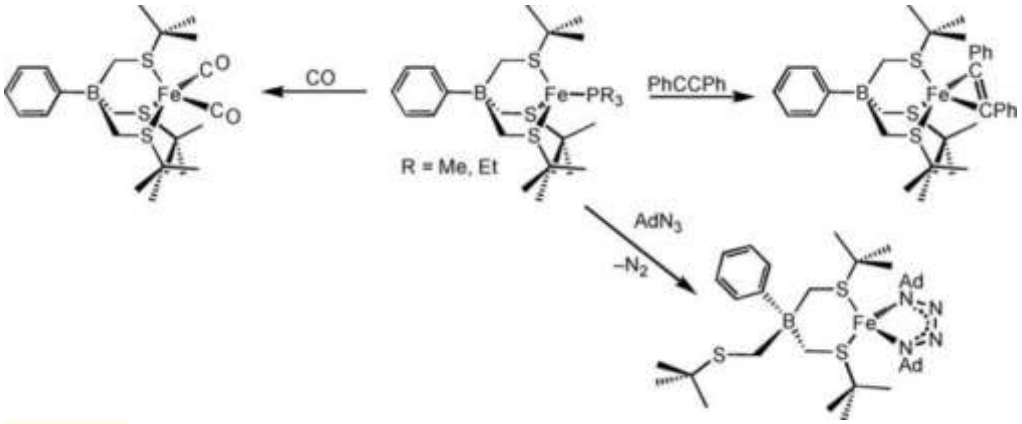

Scheme 7

Acknowledgements

I am indebted to the talents and hard work of the coworkers responsible for the development of poly(thioether)borate chemistry over the past fifteen years. Their names appear in the references cited herein. I acknowledge our collaborators, Thomas Brunold, Stephen Cramer, Codrina Popescu, and their coworkers for their expertise and numerous helpful discussions. Studies concerning ligand development, coordination and organometallic chemistry, and chalcogen activation have been funded by the National Science Foundation and the ACS-Petroleum Research Fund. The National Institutes of Health have provided financial support for studies of acetyl coenzyme A active site model complexes.

References

1. a. Caudler DL, Raymond KN. Acc. Chem. Res. 1999;32:975. [Google Scholar] b. Seidel SR, Stang PJ. Acc. Chem. Res. 2002;35:972. [PubMed] [Google Scholar]
2. Noyori R. Angew. Chem. Int. Ed. 2002;41:2008. [PubMed] [Google Scholar]
3. Dempsey JL, Esswein AJ, Manke DR, Rosenthal J, Soper JD, Nocera DG. Inorg. Chem. 2005;44:6879.[PubMed] [Google Scholar]
4. Borovik AS. Acc. Chem. Res. 2005;38:54. [PubMed] [Google Scholar]

5. Cotton FA, Wilkinson G, Murillo CA, Bochmann M. Advanced Inorganic Chemistry. sixth ed. John Wiley & Sons, Inc.; New York: 1999. p. 835. [Google Scholar]
6. Trofimenko S. Scorpionates, The Coordination Chemistry of Polypyrazolylborate Ligands. Imperial College Press; London: 1999. [Google Scholar]
7. Kitajima N, Fujisawa K, Fujimoto C, Moro-oka Y, Hashimoto S, Kitagawa T, Toriumi K, Tatsumi K, Nakamura A. J. Am. Chem. Soc. 1992;114:1277. [Google Scholar]
8. Fujisawa K, Tanaka M, Moro-oka Y, Kitajima N. J. Am. Chem. Soc. 1994;116:12079. [Google Scholar]
9. a. Shapiro IR, Jenkins DM, Thomas JC, Day MW, Peters JC. Chem. Commun. 2001:2152. [PubMed] [Google Scholar] b. Thomas JC, Peters JC. Inorg. Synth. 2004;34:8. [Google Scholar]
10. a. Kernbach U, Ramm M, Luger P, Fehlhammer WP. Angew. Chem. Int. Ed. 1996;35:310.[Google Scholar] b. Nieto I, Cervantes-Lee F, Smith JM. Chem. Commun. 2005:3811. [PubMed] [Google Scholar]
11. a. Dowling C, Murphy VJ, Parkin G. Inorg. Chem. 1996;35:2415. [PubMed] [Google Scholar] b. Hammes BS, Carrano CJ. Inorg. Chem. 1999;38:3562. [PubMed] [Google Scholar]
12. Ge PH, Haggerty BS, Rheingold AL, Riordan CG. J. Am. Chem. Soc. 1994;116:8406.[Google Scholar]
13. Garner M, Reglinski J, Cassidy I, Spicer MD, Kennedy AR. Chem. Commun. 1996:1975.[Google Scholar]
14. Trofimenko S, Calabrese JC, Thompson JS. Inorg. Chem. 1987;26:1507. [Google Scholar]
15. Kuppers HJ, Neves A, Pomp C, Ventur D, Wieghardt K, Nuber B, Weiss J. Inorg. Chem. 1986;25:2400. [Google Scholar]
16. Yim HW, Tran LM, Dobbin ED, Rabinovich D, Liable-Sands LM, Incarvito CD, Lam KC, Rheingold AL. Inorg. Chem. 1999;38:2211. [PubMed] [Google Scholar]
17. Ohrenberg C, Ge P, Schebler P, Riordan CG, Yap GPA, Rheingold AL. Inorg. Chem. 1996;35:749.[Google Scholar]
18. Ge P, Ohrenberg C, Riordan CG. Inorg. Synth. 1998;32:108. [Google Scholar]
19. Ge P, Riordan CG, Yap GPA, Rheingold AL. Inorg. Chem. 1996;35:5408. [PubMed] [Google Scholar]
20. Ge P, Rheingold AL, Riordan CG. Inorg. Chem. 2002;41:1383. [PubMed] [Google Scholar]
21. Schebler P, Riordan CG, Liable-Sands L, Rheingold AL. Inorg. Chim. Acta. 1998;270:543.[Google Scholar]
22. Chiou S-J, Ge P, Riordan CG, Liable-Sands L, Rheingold AL. Chem. Commun. 1999:159.[Google Scholar]
23. Ruth K, Tüllmann S, Vitze H, Bolte M, Lerner H-W, Holthausen MC, Wagner M. Chem. Eur. J. 2008;14:6754. [PubMed] [Google Scholar]
24. Chiou S-J, Innocent J, Lam K-C, Riordan CG, Liable-Sands L, Rheingold AL. Inorg. Chem. 2000;39:4347. [PubMed] [Google Scholar]
25. Chiou S, Riordan CG, Rheingold AL. Proc. Natl. Acad. Sci. U.S.A. 2003;100:3695. [PMC free article][PubMed] [Google Scholar]
26. Schebler PJ. Ph.D. Dissertation. University of Delaware; Newark, DE: 2000. Chemistry and Biochemistry. [Google Scholar]
27. Ge P. Masters Thesis. Kansas State University; Manhattan: 1996. Chemistry. [Google Scholar]
28. Ashby MT, Lichtenberger DL. Inorg. Chem. 1985;24:636. [Google Scholar]
29. Trofimenko S. J. Am. Chem. Soc. 1967;89:3904. [Google Scholar]
30. Piper TS, Wilkinson G. J. Inorg. Nucl. Chem. 1956;3:104. [Google Scholar]
31. Schebler PJ, Riordan CG, Guzei I, Rheingold AL. Inorg. Chem. 1998;37:4754. [PubMed] [Google Scholar]
32. Crichton O, Rest AJ. Dalton Trans. 1977:986. [Google Scholar]
33. Green JC, Underwood C. J. Organomet. Chem. 1997;528:91. [Google Scholar]
34. Landry VK, Pang K, Quan SM, Parkin G. Dalton Trans. 2007:820. [PubMed] [Google Scholar]
35. Maffett LS, Gunter KL, Kreisel KA, Yap GPA, Rabinovich D. Polyhedron. 2007;26:4758.[Google Scholar]
36. MacBeth CE, Thomas JC, Betley TA, Peters JC. Inorg. Chem. 2004;43:4645. [PubMed] [Google Scholar]

37. Nieto I, Bontchev RP, Ozarowski A, Smirnov D, Krzystek J, Telser J, Smith JM. Inorg. Chim. Acta. 2009;362:4449. [Google Scholar]
38. Ohrenberg C, Saleem MM, Riordan CG, Yap GPA, Rheingold AL. Chem. Commun. 1996:1081.[Google Scholar]
39. Ohrenberg C, Riordan CG, Liable-Sands LM, Rheingold AL. Inorg. Chem. 2001;40:4276. [PubMed] [Google Scholar]
40. Ohrenberg C, Riordan CG, Liable-Sands L, Rheingold AL. Coord. Chem. Rev. 1998;174:301.[Google Scholar]
41. Krishnan R, Voo JK, Riordan CG, Zakharov L, Rheingold AL. J. Am. Chem. Soc. 2003;125:4422.[PubMed] [Google Scholar]
42. Mirica LM, Ottenwaelder X, Stack TDP. Chem. Rev. 2004;104:1013. [PubMed] [Google Scholar]
43. Mock MT, Popescu CV, Yap GPA, Dougherty WG, Riordan CG. Inorg. Chem. 2008;47:1889.[PubMed] [Google Scholar]
44. Cho J, Yap GPA, Riordan CG. Inorg. Chem. 2007;46:11308. [PubMed] [Google Scholar]
45. DuPont JA, Yap GPA, Riordan CG. Inorg. Chem. 2008;47:10700. [PubMed] [Google Scholar]
46. Schebler PJ, Mandimutsira BS, Riordan CG, Liable-Sands L, Incarvito CD, Rheingold AL. J. Am. Chem. Soc. 2001;123:331. [PubMed] [Google Scholar]
47. DuPont JA, Mock MT, Yap GPA, Riordan CG. unpublished results.
48. Chiou SJ. Ph.D. Dissertation. University of Delaware; Newark, DE: 2004. Chemistry and Biochemistry. [Google Scholar]
49. a. Matthews RG, Goulding CW. Curr. Opin. Chem. Biol. 1997;1:332. [PubMed] [Google Scholar] b. Penner-Hahn JE. Indian J. Chem. 2002;41:13. [Google Scholar]
50. Brand U, Rombach M, Seebacher J, Vahrenkamp H. Inorg. Chem. 2001;40:6151. [PubMed] [Google Scholar]
51. Morlok MM, Janak KE, Zhu G, Quarless DA, Parkin G. J. Am. Chem. Soc. 2005;127:14039.[PubMed] [Google Scholar]
52. Warthen CR, Hammes BS, Carrano CJ, Crans DC. J. Biol. Inorg. Chem. 2001;6:82. [PubMed] [Google Scholar]
53. Maynard AT, Covell DG. J. Am. Chem. Soc. 2001;123:1047. [PubMed] [Google Scholar]
54. Smith JN, Shirin Z, Carrano CJ. J. Am. Chem. Soc. 2003;125:868. [PubMed] [Google Scholar]
55. Barondeau DP, Kassmann CJ, Bruns CK, Tainer JA, Getzoff ED. Biochemistry. 2004;43:8038.[PubMed] [Google Scholar]
56. Volbeda A, Fontecilla-Camps JC. Coord. Chem. Rev. 2005;249:1609. [Google Scholar]
57. Juan B, Thauer RK. In: Metal Ions in Life Sciences. Sigel HSA, Sigel RKO, editors. Vol. 2. Wiley; Chichester, UK: 2007. p. 323. [Google Scholar]
58. Lindahl PA, Graham DE. In: Metal Ions in Life Sciences. Sigel HSA, Sigel RKO, editors. Vol. 2. Wiley; Chichester, UK: 2007. p. 357. [Google Scholar]
59. a. Ram MS, Riordan CG, Ostrander R, Rheingold AL. Inorg. Chem. 1995;34:5884. [Google Scholar]b. Chattopadhyay S, Deb T, Ma H, Petersen JL, Young VG, Jensen MP. Inorg. Chem. 2008;47:3384.[PubMed] [Google Scholar] c. Matsunaga Y, Fujisawa K, Ibi N, Miyashita Y, Okamoto K. Inorg. Chem. 2005;44:325. [PubMed] [Google Scholar]
60. Krebs B, Henkel G. Angew. Chem. Int. Ed. 1991;30:769. [Google Scholar]
61. Cho J, Van Heuvelen KM, Yap GPA, Brunold TC, Riordan CG. Inorg. Chem. 2008;47:3913.[Google Scholar]
62. Kisko JL, Hascall T, Parkin G. J. Am. Chem. Soc. 1998;120:10561. [Google Scholar]
63. Shirasawa N, Nguyet TT, Hikichi S, Moro-oka Y, Akita M. Organometallics. 2001;20:3582.[Google Scholar]
64. Jewson JD, Liable-Sands LM, Yap GPA, Rheingold AL, Theopold KH. Organometallics. 1999;18:300. [Google Scholar]
65. Holland PL, Cundari TR, Perez LL, Eckert NA, Lachicotte RJ. J. Am. Chem. Soc. 2002;124:14416.[PubMed] [Google Scholar]
66. Shirasawa N, Akita M, Hikichi S, Moro-oka Y. Chem. Commun. 1999:417. [Google Scholar]
67. Wehmschulte RJ, Power PP. Organometallics. 1995;14:3264. [Google Scholar]
68. DuPont JA, Coxey MB, Schebler PJ, Incarvito CD, Dougherty WG, Yap GPA, Rheingold AL, Riordan CG. Organometallics. 2007;26:971. [Google Scholar]

69. Mock MT. Ph.D. Dissertation. University of Delaware; Newark, DE: 2007. Chemistry and Biochemistry. [Google Scholar]
70. Popescu CV, Mock MT, Stoian SA, Dougherty WG, Yap GPA, Riordan CG. Inorg. Chem. 2009;48:8317. [PubMed] [Google Scholar]
71. Andres H, Bominaar EL, Smith JM, Eckert NA, Holland PL, Munck E. J. Am. Chem. Soc. 2002;124:3012. [PubMed] [Google Scholar]
72. Daida EJ, Peters JC. Inorg. Chem. 2004;43:7474. [PubMed] [Google Scholar]
73. DuPont JA. Ph.D. Dissertation. University of Delaware; Newark, DE: 2005. Chemistry and Biochemistry. [Google Scholar]
74. Mandimutsira BS, Riordan CG, Rheingold AL. unpublished results.
75. Fujita K, Rheingold AL, Riordan CG. J. Chem. Soc., Dalton Trans. 2003:2004. [Google Scholar]
76. George SJ, Seravalli J, Ragsdale SW. J. Am. Chem. Soc. 2005;127:13500. [PubMed] [Google Scholar]
77. Craft JL, Mandimutsira BS, Fujita K, Riordan CG, Brunold TC. Inorg. Chem. 2003;43:859. [PubMed] [Google Scholar]
78. Detrich JL, Konecny R, Vetter WM, Doren D, Rheingold AL, Theopold KH. J. Am. Chem. Soc. 1996;118:1703. [Google Scholar]
79. Popescu CV, Munck E. J. Am. Chem. Soc. 1999;121:7877. [Google Scholar]
80. Mehn MP, Peters JC. J. Inorg. Biochem. 2006;100:634. [PubMed] [Google Scholar]
81. a. Nieto I, Ding F, Bontchev RP, Wang HB, Smith JM. J. Am. Chem. Soc. 2008;130:2716. [PubMed] [Google Scholar] b. Scepaniak JJ, Fulton MD, Bontchev RP, Duesler EN, Kirk ML, Smith JM. J. Am. Chem. Soc. 2008;130:10515. [PubMed] [Google Scholar]
82. Trogler WC. Acc. Chem. Res. 1990;23:426. [Google Scholar]
83. Cowley RE, Bill E, Neese F, Brennessel WW, Holland PL. Inorg. Chem. 2009;48:4828. [PubMed] [Google Scholar]
84. Mandimutsira BS, Yamarik JL, Brunold TC, Gu W, Cramer SP, Riordan CG. J. Am. Chem. Soc. 2001;123:9194. [PubMed] [Google Scholar]
85. Schenker R, Mandimutsira BS, Riordan CG, Brunold TC. J. Am. Chem. Soc. 2002;124:13842.[PubMed] [Google Scholar]
86. Fujita K, Schenker R, Gu W, Brunold TC, Cramer SP, Riordan CG. Inorg. Chem. 2004;44:3324. [PubMed] [Google Scholar]
87. Aboelella NW, Kryatov SV, Gherman BF, Brennessel WW, Young VG, Jr., Sarangi R, Rybak-Akimova EV, Hodgson KO, Hedman B, Solomon EI, Cramer CJ, Tolman WB. J. Am. Chem. Soc. 2004;126:16896. [PubMed] [Google Scholar]
88. Betley TA, Peters JC. Inorg. Chem. 2003;42:5074. [PubMed] [Google Scholar]
89. Hu X, Meyer K. J. Am. Chem. Soc. 2004;126:16322. [PubMed] [Google Scholar]
90. Aboelella NW, York JT, Reynolds AM, Fujita K, Kinsinger CR, Cramer CJ, Riordan CG, Tolman WB. Chem. Commun. 2004:1716. [PubMed] [Google Scholar]
91. Fujisawa K, Moro-oka Y, Kitajima N. J. Chem. Soc., Chem. Commun. 1994:623. [Google Scholar]